XLIII CILAMCE
21–25, November, 2022
FOZ DO IGUAÇU – PR – BRAZIL

2D contact simulation of fretting specimens using IGABEM

L. B. Silva[1], F. M. Loyola[1], T. Doca[1], E. L. Albuquerque[1]

[1]*ENM – Department of Mechanical Engineering, Faculty of Technology, University of Brasília*
Campus Darcy Ribeiro, 70910-900, Brasília, DF – Brazil
leobsilvaa@gmail.com, f.loyola91@gmail.com, doca@unb.br, eder@unb.br

Abstract. In this paper, the isogeometric boundary element method (IGABEM) is used for determining tractions in contact problems. We simulate contact between a fretting pad and a metallic specimen, a usual experimental configuration. The results are compared with standard boundary elements method and analytical results. The analysis consists of evaluating tractions during one loading cycle, which includes normal and shear loads. After, the results are validated using analytical formulae. Lastly, a performance comparison between each method is presented.

Keywords: Fretting Fatigue, Contact Problems, Isogeometric Boundary Element Method.

1 Introduction

Fretting fatigue by Waterhouse and Lindley [1] is a failure process observed in contact surfaces under cyclical loading. It is regarded as the main cause of failure in several mechanical systems (i.e., dovetail joints, wire cables, threaded pipe connections, bolted and riveted joints) and can represent a considerable cost in terms of a country's GNP by Reed et al. [2]. Moreover, high strength aluminium and titanium are often the material of choice in components susceptible to fretting fatigue. They are costly and difficult to machine. Therefore, cost-efficient methods for the life estimation of components are paramount.

Although finite elements are the most used numerical method for the analysis of fretting problems, Boundary Element based approaches have some interesting features that should be taken into account. An analysis using BEM requires less cost associated with the discretization of the problem. Moreover, BEM meshes can be extremely easy to generate, specially when using an Isogeometrical approach.

Isogeometric analysis (IGA) [3, 4] uses the same functions for modelling the geometry and for approximating the unknown fields in numerical analysis. Although it is possible to develop isogeometric methods based on T-Splines [5–7] or others, the most common is based on Non-Uniform Rational B-Splines (NURBS). They are a standard for curve and surface representation in Computer-Aided Design (CAD) systems and have features such as representing exactly all conic sections and being refined by knot insertion.

In this work, the IGABEM is used for analysis of two-dimensional elastic contact problems under a fretting fatigue loading condition. Normal and shear stresses at contact region are compared to analytical solutions in different moments of the cyclic load. Very accurate results are obtained. A comparison made with the conventional BEM [8], using Lagrangian polynomials as basis function, has shown that the IGABEM is more accurate if we consider the same number of degrees of freedom.

1.1 IGABEM

The main difference between IGABEM and the conventional BEM is that the former uses Non-uniform rational B-splines (NURBS) as basis functions to approximate the geometry and unknown boundary fields. In IGABEM, the definition of element is not as straightforward as in the conventional formulation. Due to that, after discretizing the boundary, the physical domain is mapped to a parameter element $[\xi_i, \xi_j]$ which is the interval between two consecutive unique knots.

Interpolating geometry and unknown variables using NURBS, we have:

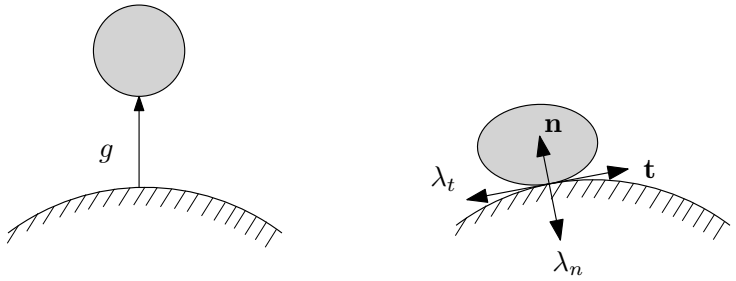

Figure 1. Bodies separated by an initial gap (left) and establishment of a contact condition (right).

$$x_j(\xi) = \sum_1^n R_{i,p}(\xi) x_c, \tag{1}$$

$$u_j(\xi) = \sum_1^n R_{i,p}(\xi) u_c, \tag{2}$$

$$t_j(\xi) = \sum_1^n R_{i,p}(\xi) t_c, \tag{3}$$

where $R_{i,p}$ are defined as

$$R_{i,p}(\xi) = \frac{N_{i,p}(\xi) w_i}{\sum_{j=1}^n N_{j,p}(\xi) w_j}. \tag{4}$$

$N_{i,p}(\xi)$ is the ith B-spline basis functions of degree p [9], x_c is the coordinate of a control point and u_c and t_c are displacements and tractions coefficients, respectively. Each one of the previous coefficients are associated with a control point. Attention is needed because those values do not have a physical meaning, as the control point might lie outside the boundary. In order to recover displacements and tractions associated with collocation points over the boundary, we can do the following:

$$\mathbf{u} = \mathbf{E}\mathbf{u_c} \tag{5}$$

$$\mathbf{t} = \mathbf{E}\mathbf{t_c} \tag{6}$$

where $\mathbf{E}$ is a transformation matrix defined in [10, 11].

2 Contact formulation

A classical depiction of a contact process is given in Fig. 1. It encompasses two basic stages: 1) the evaluation of the normal gap, g, between the contacting surfaces; and 2) the calculation of the contact pressure, λ_n, whenever the normal gap is closed.

This relationship is often denoted as the Kuhn-Karush-Tucker condition,

$$\begin{aligned} g &\geq 0, \\ \lambda_n &\leq 0, \\ \lambda_n g &= 0. \end{aligned} \tag{7}$$

Moreover, the contact conditions can be thought as constraints that must be satisfied for each node-pair within the contact zone. Therefore, they can be defined into three states:

- **Separated** is when both nodes are within a positive and non-zero distance from each other.
- **Stick** bodies are in contact while not displaying tangential motion.
- **Slip** bodies are in contact and without restriction in the tangential direction.

Table 1 lists the relationships that represent the three modes of contact previously stated, where t_n and t_t are the normal and tangential tractions, and u_n and u_t are the normal and tangential displacements (expressed in local coordinates), respectively. It is important to remark that state of the node-pairs is continuously updated within the iterative procedure.

Table 1. Set of traction/displacement relations for the contact conditions.

Separated	**Stick**	**Slip**
$t_t^a - t_t^b = 0$	$t_t^a - t_t^b = 0$	$t_t^a - t_t^b = 0$
$t_n^a - t_n^b = 0$	$t_n^a - t_n^b = 0$	$t_n^a - t_n^b = 0$
$t_t^a = 0$	$u_t^a - u_t^b = 0$	$t_t^a \pm \mu t_n^a = 0$
$t_n^a = 0$	$u_n^a - u_n^b = g^{ab}$	$u_n^a - u_n^b = g^{ab}$

The proposed formulation addresses frictional contact in a two-dimensional setting. The solids are regarded as homogeneous isotropic linear elastic bodies. For instance, let us consider the bodies A and B so that their deformations can be described by two coupled integral equations, one for each body, as follows,

$$c_{ij}^A u_j^A + \sum_{n=1}^{N_A} H_{ij}^A u_j^A = \sum_{n=1}^{NA} G_{ij}^A t_j^A \tag{8}$$

$$c_{ij}^B u_j^B + \sum_{n=1}^{N_B} H_{ij}^B u_j^B = \sum_{n=1}^{NB} G_{ij}^B t_j^B \tag{9}$$

where N_A and N_B are the number of collocation points of bodies A and B, respectively. Therefore, two sets of linear equations are obtained and their matrix form, can be written such that,

$$[H]^\gamma \{u\}^\gamma = [G]^\gamma \{t\}^\gamma \ , \ \gamma = A, B \tag{10}$$

As noted by [12, 13], for linear problems, once this system of equations has been solved, the final solution for displacements and tractions everywhere on the boundaries can be obtained. This is not the case for this study, as we are dealing with a non-linear problem. This non-linearity comes from the fact that the contact region is not known *a priori* and it must be determined as part of the solution. In order to overcome this, the same approach used in [8, 14, 15] is reproduced here. It consists of an iterative method known as generalized Newton's method.

3 Numerical analysis

This section presents a numerical analysis of the Cattaneo-Mindlin problem to assess the accuracy of the proposed IGABEM formulation. The accuracy is assessed via comparison with analytical solutions [16–19] and a comparison to an conventional BEM using continuous quadratic elements.

3.1 Cattaneo-Mindlin problem

The Cattaneo-Mindlin problem is shown in Fig. 2. It consists of two elastically-similar bodies in frictional contact. The body is loaded with a normal force and a tangential force while restricted at its central node in the $x-$direction. The body 2 is fully restrained on its bottom.

Firstly, a normal load is applied. Then, this load is maintained constant while a tangential load is cyclically applied. A depiction of the loading scheme is shown in Fig. 3.

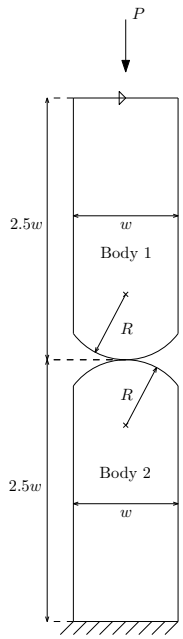

Figure 2. Cattaneo-Mindlin - problem configuration.

As the two bodies have similar geometries, they are discretized with the same mesh. In order to compare results from conventional BEM and IGABEM, the mesh is discretized in a way that both have the same number of node-pairs in the contact zone, i.e., $NP_c = 61$.

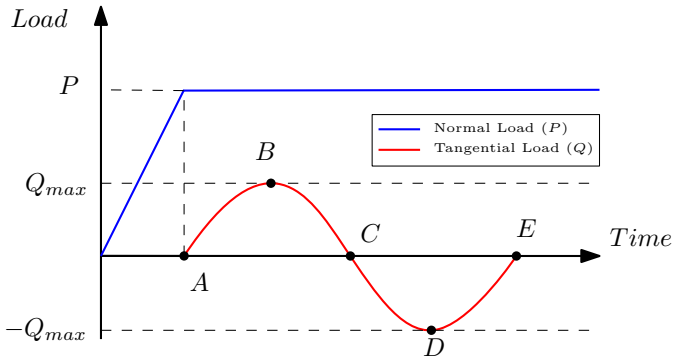

Figure 3. Cattaneo-Mindlin - loading scheme containing five steps (A-E).

Point A is when the normal load P reaches its final value, whereas point B is the moment when the maximum tangential load is applied. Afterwards, tangential load starts to decrease, passing through zero at point C and decreasing further. Point D is when the tangential load is in its minimum value and, finally, point E is when the tangential load reaches zero again. Geometric and material properties can be seen in Table 2.

Table 2. Cattaneo-Mindlin - Dimensions and material properties.

Property	**Symbol**	**Value**
Radius	R	70 mm
Length	w	6.5 mm
Young's Modulus	E	73.4 GPa
Poisson's ratio	ν	0.33
Pressure	P	100 N/mm
Friction coefficient	f	0.3

In this problem, both BEM and IGABEM have a finer mesh in segments that may be in contact.

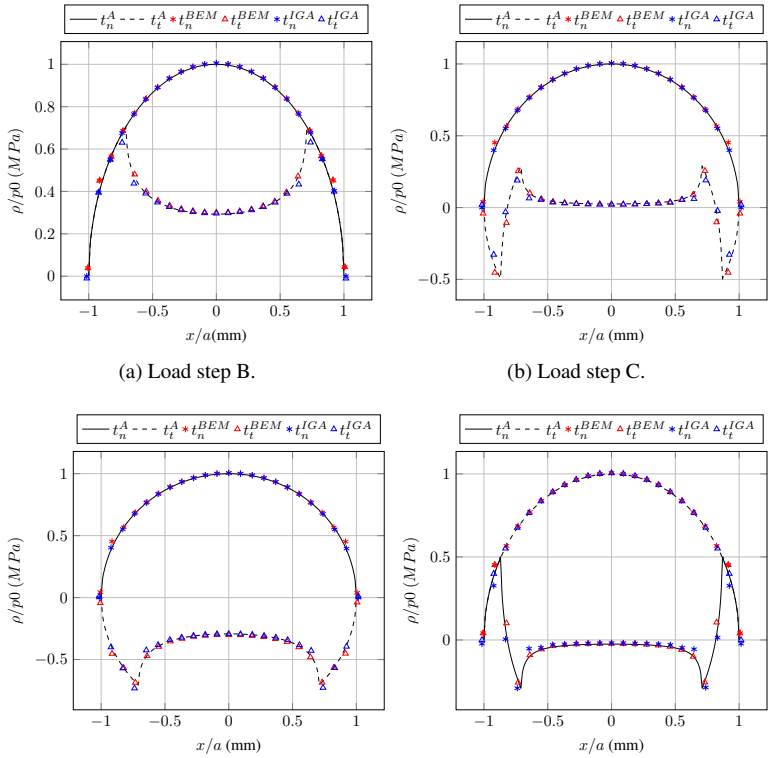

(a) Load step B.

(b) Load step C.

(c) Load step D.

(d) Load step E.

Figure 4. Cattaneo-Mindlin - normal (t_n) and tangential (t_t) tractions comparison of IGABEM, BEM and analytical results at four load steps (B-E).

3.2 Tractions

Fig's. 4a- 4d compare the tractions of conventional BEM and IGABEM with the analytical solution for four out of five loading steps, B to E. Both normal and tangential tractions for BEM (t_n^{BEM} and t_t^{BEM}), IGABEM (t_n^{IGA} and t_t^{IGA}) and analytical solutions (t_n^A and t_t^A) are shown.

The vertical dimension of the two bodies is large enough ($2.5w$) to provide no tangential load in the first step, as demanded by the analytical solution. So, $\mathbf{t}_t \approx \mathbf{0}$ in the first step.

3.3 Displacements

Displacements fields in normal and tangential directions were measured and their results are presented in this section. Figures (5a-5d) compare the displacements for BEM and IGABEM for load steps 2 to 5.

Only the displacements of node-pairs within the contact zone are shown. Although there is no analytical solution to compare with, we can see that there is a good agreement between the two methods.

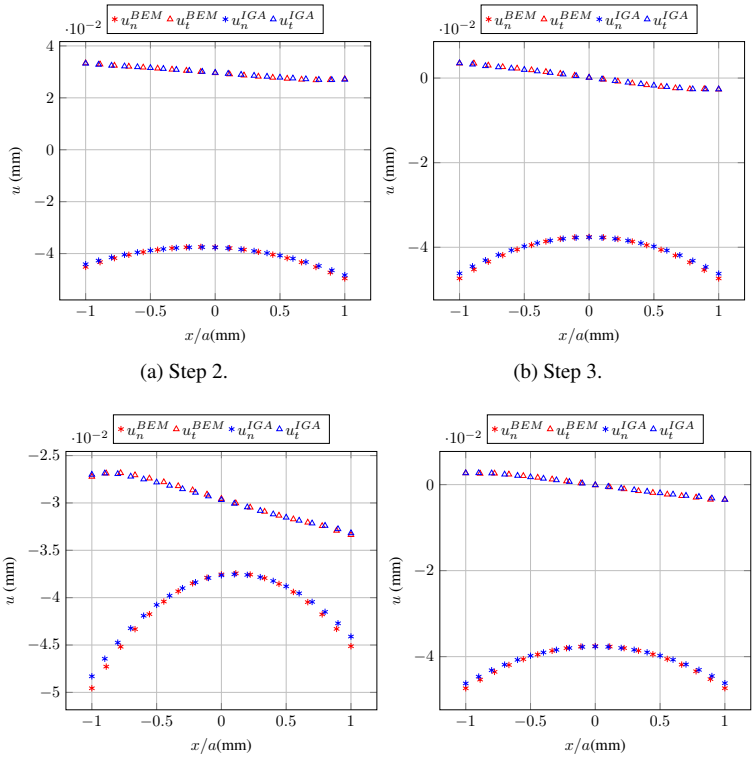

(a) Step 2. (b) Step 3.

(c) Step 4. (d) Step 5.

Figure 5. Cattaneo-Mindlin - IGABEM and BEM normal (u_n) and tangential (u_t) displacements fields over contact surface for load steps (B-E).

It can be seen that the results are in good agreement. The maximum error is 4.104 % for shear tractions localized in the frontier of the slip-stick region. In all other points, all curves are very near. Normal tractions remain the same during the load steps while tangential tractions change.

4 Conclusions

This paper presented an extension of the IGABEM to the analysis of contact problems under cyclic loads. Details of the formulation are shown and its accuracy is assessed throughout comparison with the isoparametric quadratic continuous boundary elements and analytical solutions showing good agreement. One of main advantages of the use of IGABEM in contact problems is that it can exactly represent the contact surface with few control points. Thus, we can have accurate solutions with few degrees of freedom.

Acknowledgements. The authors gratefully acknowledge the financial support provided by the Brazilian National Council for Scientific and Technological Development (CNPq), the Foundation for the Support of Research in the Federal District (FAP-DF) and the Brazilian Federal Agency for Support and Evaluation of Graduate Education (CAPES) - Finance Code 001.

Authorship statement. The authors hereby confirm that they are the sole liable persons responsible for the authorship of this work, and that all material that has been herein included as part of the present paper is either the property (and authorship) of the authors, or has the permission of the owners to be included here.

References

[1] R. B. Waterhouse and T. C. Lindley. *Fretting fatigue*. John Wiley & Sons, 1994.
[2] R. P. Reed, J. H. Smith, and B. W. Christ. The economic effects of fracture in the united states. *U.S. Dept. of Commerce,*, vol. , pp. 19, 1983.

[3] T. Hughes, J. Cottrell, and y. Bazilevs. Isogeometric analysis: CAD, finite elements, NURBS, exact geometry and mesh refinement. *Computer Methods in Applied Mechanics and Engineering*, vol. 194, n. 39-41, pp. 4135–4195, 2005.
[4] A. Cottrell, T. Hughes, and Y. Bazilevs. *Isogeometric Analysis: Toward Integration of CAD and FEA*. Wiley, 2009.
[5] Y. Bazilevs, V. Calo, J. Cottrell, J. Evans, T. Hughes, S. Lipton, M. Scott, and T. Sederberg. Isogeometric analysis using t-splines. *Computer Methods in Applied Mechanics and Engineering*, vol. 199, n. 5-8, pp. 229–263, 2010.
[6] M. A. Scott, M. J. Borden, C. V. Verhoosel, T. W. Sederberg, and T. J. R. Hughes. Isogeometric finite element data structures based on bézier extraction of t-splines. *International Journal for Numerical Methods in Engineering*, vol. 88, n. 2, pp. 126–156, 2011.
[7] R. Dimitri, L. D. Lorenzis, M. Scott, P. Wriggers, R. Taylor, and G. Zavarise. Isogeometric large deformation frictionless contact using t-splines. *Computer Methods in Applied Mechanics and Engineering*, vol. 269, pp. 394–414, 2014.
[8] B. M. Cavalcante, M. H. Shaterzadeh-Yazdi, P. Sollero, E. L. Albuquerque, and T. Doca. Analysis of a Cattaneo-Mindlin problem using the Boundary Element Method. *Trib. Int.*, vol. 108, pp. 194–201, 2017.
[9] F. M. Loyola, T. Doca, L. S. Campos, J. Trevelyan, and E. L. Albuquerque. Analysis of 2D contact problems under cyclic loads using IGABEM with Bézier decomposition. *Eng. Anal. Bound. Elem.*, vol. 139, pp. 246–263, 2022.
[10] J. Cabral, L. Wrobel, and C. Brebbia. A BEM formulation using b-splines: I-uniform blending functions. *Engineering Analysis with Boundary Elements*, vol. 7, n. 3, pp. 136–144, 1990.
[11] J. Cabral, L. Wrobel, and C. Brebbia. A BEM formulation using b-splines: II-multiple knots and non-uniform blending functions. *Engineering Analysis with Boundary Elements*, vol. 8, n. 1, pp. 51–55, 1991.
[12] K. Man, M. Aliabadi, and D. Rooke. Bem frictional contact analysis: Load incremental technique. *Computers & Structures*, vol. 47, n. 6, pp. 893–905, 1993a.
[13] K. Man, M. Aliabadi, and D. Rooke. BEM frictional contact analysis: Modelling considerations. *Engineering Analysis with Boundary Elements*, vol. 11, n. 1, pp. 77–85, 1993b.
[14] L. Rodríguez-Tembleque and R. Abascal. A FEM–BEM fast methodology for 3d frictional contact problems. *Computers & Structures*, vol. 88, n. 15-16, pp. 924–937, 2010.
[15] L. Rodríguez-Tembleque, F. García-Sánchez, and A. Sáez. Crack-face frictional contact modelling in cracked piezoelectric materials. *Computational Mechanics*, vol. 64, n. 6, pp. 1655–1667, 2019.
[16] D. Hills. *Mechanics of elastic contacts*. Butterworth-Heinemann, Oxford England Boston, 1993.
[17] D. A. Hills. *Mechanics of Fretting Fatique*. Springer Netherlands, Dordrecht, 1994.
[18] K. L. Johnson. *Contact Mechanics*. Cambridge University Press, 2004.
[19] V. Popov. *Contact mechanics and friction : physical principles and applications*. Springer, Heidelberg New York, 2010.